Parametric Continuous-Time Blind System Identification

Document status and date:
Published: 19/01/2024

Document Version:
Accepted manuscript including changes made at the peer-review stage

Please check the document version of this publication:

• A submitted manuscript is the version of the article upon submission and before peer-review. There can be important differences between the submitted version and the official published version of record. People interested in the research are advised to contact the author for the final version of the publication, or visit the DOI to the publisher's website.
• The final author version and the galley proof are versions of the publication after peer review.
• The final published version features the final layout of the paper including the volume, issue and page numbers.

Link to publication

Parametric Continuous-Time Blind System Identification

Augustus Elton[1], Rodrigo A. González[2], James S. Welsh[1], Cristian R. Rojas[3], Minyue Fu[1]

Abstract— In this paper, the blind system identification problem for continuous-time systems is considered. A direct continuous-time estimator is proposed by utilising a state-variable-filter least squares approach. In the proposed method, coupled terms between the numerator polynomial of the system and input parameters appear in the parameter vector which are subsequently separated using a rank-1 approximation. An algorithm is then provided for the direct identification of a single-input single-output linear time-invariant continuous-time system which is shown to satisfy the property of correctness under some mild conditions. Monte Carlo simulations demonstrate the performance of the algorithm and verify that a model and input signal can be estimated to a proportion of their true values.

I. INTRODUCTION

System identification [1] considers the problem of obtaining a mathematical model for a process using input and output data. It is classified as blind system identification (BSI) or blind equalisation (BE) when the user is *blind* to the input, that is, they cannot take direct input measurements. BSI and BE approaches have been used in fields such as communications [2], [3], image processing [4], and biomedical science [5]. Survey papers [6] and [7] provide an introduction to BSI and a brief overview of some approaches.

In BSI, identifiability conditions are established so that an appropriate model of the system can be realised. To identify a system using a parametric transfer function it is typical to assume that the numerator and denominator polynomials are co-prime, and that the input excitation is persistently exciting [1]. However, in the blind problem, extra conditions formed from prior system or input knowledge are required as the identification problem is ill posed in general. As an example, an infinite impulse response model can be recovered provided that the input is oversampled and applied to the system using a zero-order hold (ZOH) [3]. Within the area of BSI, a system is considered to be blindly identifiable if the obtained model is an accurate representation of the true system, up to a constant gain [6].

In this paper, we propose a direct blind continuous-time (CT) method that allows the input to be described by a linear combination of continuous-time functions and the system as a rational transfer function of two polynomials.

Directly identifying the system in CT allows the user to consider systems with rapid or irregular sampling [8], [9]. Additionally, a CT model can provide physically meaningful values of the system parameters.

To the best of the authors' knowledge there are no blind approaches for single-input single-output (SISO) systems which establish a parametric CT model directly, i.e. without the use of intermediate discrete-time models. In this paper we broaden the underlying input assumption and produce the CT estimate *directly* by using a least squares state variable filter (LSSVF) approach [10]. Similar approaches to identify the input sequence include subspace methods [3], [11]. In summary, the main contributions of this paper are:

(C1) We derive a blind, direct CT estimator for a linear time-invariant (LTI) SISO system, by
   a) proposing a CT estimator of the denominator polynomial and coupled parameters between the numerator coefficients and input parameters using a state variable filter least squares approach, and
   b) separating the coupled terms to form an input and transfer function estimate of the system.
(C2) We propose an algorithm where we
   a) show that it satisfies the correctness property [15], and
   b) evaluate its performance numerically through Monte Carlo simulations.

The remainder of this paper is organised as follows. Section II introduces the problem formulation and blind system identification. Section III provides the derivations for the blind form of the least squares state variable filter approach and states the algorithm. Section IV provides simulations and results of the blind estimator. Conclusions are deduced in Section V.

II. PROBLEM STATEMENT

We consider a linear time-invariant, continuous-time, single-input single-output system

$$\mathcal{S} : \begin{cases} x(t) = \frac{B(p)}{A(p)} u(t) \\ y(t) = x(t) + v(t), \end{cases} \tag{1}$$

where $u(t)$ is the input and $x(t)$ is the noise-free output. The output, $y(t)$, is $x(t)$ corrupted by an output measurement noise $v(t)$. The output measurement noise is assumed to be a zero-mean Gaussian process, i.e. $v(t) \sim N(0, \sigma^2)$. The system $B(p)/A(p)$ is assumed to be a rational transfer function with numerator and denominator polynomial of orders m and n, given by

$$B(p) = b_m p^m + b_{m-1} p^{m-1} + \cdots + b_0, \tag{2}$$

$$A(p) = p^n + a_{n-1} p^{n-1} + \cdots + a_0, \tag{3}$$

respectively, where the differentiation operator $p = d/dt$ is used to denote that the system is in continuous-time. The system is assumed to be causal ($n \geq m$) and the polynomials of (2) and (3) are co-prime, i.e. there are no common pole and zero pairs. The parameter vector used to describe the true system (1) is

$$\boldsymbol{\theta}^* := [a_{n-1}^*, \ldots, a_1^*, a_0^*, b_m^*, \ldots, b_1^*, b_0^*]^\top. \quad (4)$$

The true system is then given by

$$G^*(p) = \frac{B^*(p)}{A^*(p)}, \quad (5)$$

where $B^*(p)$ and $A^*(p)$ are formed from (2) and (3) using the parameter vector (4). The system and signals are shown in Fig. 1, where data is acquired by sampling the output signal at time instances $t \in \{t_1, t_2, \ldots, t_N\}$.
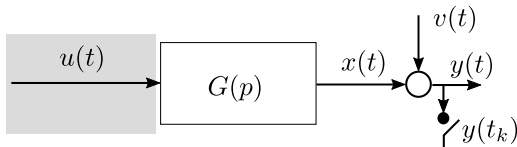

Fig. 1. Block diagram of the CT system. Note that the opaque grey box indicates that the user does not have access to the input.

The goal of BSI is to obtain a model of the system, $G(p)$, and an accurate representation of the input, $u(t)$, by only using the sampled output data $\{y(t_k)\}_{k=1}^N$. Our aim is to provide an estimate of the input sequence $\{u(t_k)\}_{k=1}^N$ and an estimate of the parametric model in (5) up to a scalar constant of the true system using a direct CT method. To identify the system uniquely, we assume that the unknown input can be described by a linear combination of continuous-time functions which are known. For clarity, we denote $\boldsymbol{\theta}^*$ and $\hat{\boldsymbol{\theta}}$ as the true and estimated parameter vector of the model, respectively.

III. BLIND SYSTEM IDENTIFICATION

In BSI we do not have access to the input and, therefore, common CT approaches in system identification are not viable. In this section we propose a blind form of the least squares state variable filter [12], that we denote as the BLSSVF approach, which corresponds to contribution (C1.a). Here, the input is assumed to be described by a continuous-time function with the general form

$$u(t) = \sum_{i=1}^M \gamma_i h(t - \tau_i), \qquad \text{for } M \in \mathbb{N}, \quad (6)$$

where τ_i and γ_i are the ith translation and magnitude of a fixed signal $h(t)$, respectively. In the sequel, we state the assumptions on the input that are necessary to develop the proposed blind estimator.

Assumption 3.1: The specified translations $\{\tau_i\}_{i \geq 1}$ occur regularly over a period of T_u seconds.

Assumption 3.2: The true input can be described by (6), given the true values of γ for some functions of $h(t)$ which admit the true input intersample behaviour. The function $h(t)$ is provided by the user.

Using Assumption 3.1 and knowing the number of samples, N, then $M = NT_s/T_u$, where T_s is the output sampling period. Typically, the input of the system undergoes a signal reconstruction modelled by a digital to analog conversion. This process is modelled where the exact intersample behaviour of the input is assumed [14]. The digital to analog process can be used to set $h(t)$. For example, consider that the input, $u(t)$, into the physical system is constructed by a ZOH. Then, the input can be described by

$$u(t) = \sum_{i=1}^M \gamma_i \mu(t - \tau_i), \quad (7)$$

where $\mu(t)$ is the unit step function and the parameters $[\gamma_1, \gamma_2, \ldots, \gamma_M]$ represent the change in magnitude between each step. Given the relationship in (6), the model $\mathcal{M}$ for the digital implementation of BLSSVF can be written as

$$\mathcal{M} : \begin{cases} x(t_k) = \left\{ \frac{B(p)}{A(p)} \cdot \sum_{i=1}^M \gamma_i h(t - \tau_i) \right\}_{t=t_k}, \\ y(t_k) = x(t_k) + \epsilon(t_k). \end{cases} \quad (8)$$

The underlying mechanism for determining a suitable estimator is to form a regression equation from (8) given sampled data $\{y(t_k)\}_{k=1}^N$. Inspired by the CT approaches in e.g., [14], we can form a generalised error equation for the blind case in (8),

$$\epsilon(t_k) = y(t_k) - x(t_k)$$
$$= \frac{1}{A(p)} \left(A(p)y(t_k) - B(p) \sum_{i=1}^M \gamma_i h(t_k - \tau_i) \right), \quad (9)$$

which is used to create the input-output equation

$$(p^{(n)} + a_{n-1}p^{(n-1)} + \ldots + a_0)y_f(t_k) =$$
$$(b_m p^{(m)} + b_{m-1}p^{(m-1)} + b_0) \sum_{i=1}^M \gamma_i h_f(t_k - \tau_i) + \epsilon(t_k), \quad (10)$$

where

$$y_f^{(l)}(t_k) = \frac{p^{(l)}}{A(p)} y(t_k), \text{ and } h_f^{(l)}(t_k) = \frac{p^{(l)}}{A(p)} h(t_k). \quad (11)$$

Rearranging (10) in terms of $y_f^{(n)}(t_k)$ yields

$$y_f^{(n)}(t_k) = -\sum_{i=0}^{n-1} a_i y_f^{(i)}(t_k) + \sum_{i=0}^m b_i \mathbf{c}^\top \mathbf{h}_f^{(i)}(t_k) + \epsilon(t_k), \quad (12)$$

where

$$\mathbf{h}_f^{(i)}(t_k) = \left[h_f^{(i)}(t_k - \tau_1), h_f^{(i)}(t_k - \tau_2), \ldots, h_f^{(i)}(t_k - \tau_M) \right]^\top, \quad (13)$$
$$\mathbf{c} = [\gamma_1, \gamma_2, \ldots, \gamma_M]^\top. \quad (14)$$

It can be seen that (12) cannot be used to describe a residual equation that is linear in the parameters, since coupled products exist between the numerator polynomial coefficients $\mathbf{b} = [b_m, \ldots, b_1, b_0]^\top$, and the input parameters, $\mathbf{c}$. Now, let us consider an extended parameter vector

$$\boldsymbol{\theta} = [\mathbf{a}^\top, \mathbf{z}_m^\top, \ldots, \mathbf{z}_1^\top, \mathbf{z}_0^\top]^\top \in \mathbb{R}^{n+(m+1)M}, \quad (15)$$

where $\mathbf{a} = [a_{n-1}, \ldots, a_1, a_0]^\top$, and
$$\mathbf{z}_i = [b_i \gamma_1, \ldots, b_i \gamma_{M-1}, b_i \gamma_M]^\top.$$

Using the parameter vector (15) we have

$$y_f^{(n)}(t_k) = \varphi_f^\top(t_k)\boldsymbol{\theta} + \epsilon(t_k), \quad (16)$$

where the regressor is constructed using (11) and (13)

$$\varphi_f(t_k) = \left[-y_f^{(n-1)}(t_k), -y_f^{(n-2)}(t_k), \dots, -y_f^{(0)}(t_k), \right.$$
$$\left. \mathbf{h}_f^{(m)}(t_k), \mathbf{h}_f^{(m-1)}(t_k), \dots, \mathbf{h}_f^{(0)}(t_k) \right]^\top . \quad (17)$$

To form (16), (11) must be computed. The input and output time derivatives are computed using a state variable filter [12] $F(p)$, i.e.

$$y_f^{(l)}(t_k) = \frac{p^{(l)}}{F(p)} y(t_k), \text{ and } h_f^{(l)}(t_k) = \frac{p^{(l)}}{F(p)} h(t_k). \quad (18)$$

The filter $F(p)$ has the form

$$F(p, \lambda_{SVF}) = \left(\frac{p}{\lambda_{SVF}} + 1 \right)^n, \quad (19)$$

where λ_{SVF} is selected to ensure that $F(p)$ has a larger bandwidth than that of the system [10]. Utilising N output data samples, minimising the squared error term in (16) yields the least squares solution

$$\hat{\boldsymbol\theta} = \left[\frac{1}{N} \sum_{k=1}^N \varphi_f(t_k)\varphi_f(t_k)^\top \right]^{-1} \left[\frac{1}{N} \sum_{k=1}^N \varphi_f(t_k) y_f^{(n)}(t_k) \right]. \quad (20)$$

In matrix form we have

$$\hat{\boldsymbol\theta} = (\boldsymbol\varphi^\top \boldsymbol\varphi)^{-1} \boldsymbol\varphi^\top \mathbf{y}_f, \quad (21)$$

where

$$\boldsymbol\varphi = [\varphi_f(t_1), \varphi_f(t_2), \dots, \varphi_f(t_N)]^\top \in \mathbb{R}^{N \times (n+(m+1)M)}, \quad (22)$$

and

$$\mathbf{y}_f = [y_f^{(n)}(t_1), y_f^{(n)}(t_2), \dots, y_f^{(n)}(t_N)]^\top \in \mathbb{R}^{N \times 1}. \quad (23)$$

To obtain $\hat{\boldsymbol\theta}$, the normal matrix $(\boldsymbol\varphi^\top \boldsymbol\varphi)$ must be nonsingular, which requires $N \geq n + (m+1)M$. An issue arising from (15) that needs to be addressed, concerns the coupled products between $\mathbf{b}$ and $\mathbf{c}$ are contained in the vector $\mathbf{z}$. To address this issue, related to contribution (C1.b), we use a rank-1 approximation. Consider the matrix

$$\mathbf{Z} = [\mathbf{z}_m, \mathbf{z}_{m-1}, \dots, \mathbf{z}_0]^\top \in \mathbb{R}^{(m+1) \times M}. \quad (24)$$

The rank-1 approximation of $\mathbf{b}$ and $\mathbf{c}$ is then

$$[\hat{\mathbf{b}}, \hat{\mathbf{c}}] = \underset{\mathbf{b} \in \mathbb{R}^{(m+1) \times 1}, \mathbf{c} \in \mathbb{R}^{M \times 1}}{\arg\min} \|\mathbf{Z} - \mathbf{b}\mathbf{c}^\top\|_F^2, \quad (25)$$

where $\| \cdot \|_F$ denotes the Frobenius norm of a matrix. The rank-1 approximation can be performed via the singular value decomposition (SVD)

$$\mathbf{Z} = \mathbf{U}\boldsymbol\Sigma\mathbf{V}^\top, \quad (26)$$

where $\mathbf{U} \in \mathbb{R}^{(m+1) \times (m+1)}$ and $\mathbf{V} \in \mathbb{R}^{M \times M}$ contain the left and right singular vectors of $\mathbf{Z}$, respectively, with the singular values

$$\boldsymbol\Sigma = \begin{bmatrix} \sigma_1 & 0 & \dots & 0 \\ 0 & \sigma_2 & \dots & 0 \\ \vdots & \vdots & \ddots & \vdots \end{bmatrix} \in \mathbb{R}^{(m+1) \times M}. \quad (27)$$

The outer product of the first column vectors of the singular matrices $\mathbf{U}$ and $\mathbf{V}$, which are associated with the largest

singular value, σ_1, are used to form a rank-1 approximation of $\mathbf{Z}$. These vectors correspond to the estimates

$$\hat{\mathbf{b}} = \mathbf{U}_{(:,1)}\sigma_1, \text{ and } \hat{\mathbf{c}} = \mathbf{V}_{(:,1)}, \quad (28)$$

where $\mathbf{U}_{(:,1)}$ and $\mathbf{V}_{(:,1)}$ denote the first column of the matrices $\mathbf{U}$ and $\mathbf{V}$, respectively. The fit of the approximation

$$\text{R-1 Fit} = \frac{\sigma_1}{\sum_{i=1}^{\min\{m+1,M\}} \sigma_i}, \quad (29)$$

is used to assess how well the vectors $\hat{\mathbf{b}}$ and $\hat{\mathbf{c}}$ describe the estimate of $\mathbf{Z}$ obtained from (21). Finally we can form the estimates of the model and the input

$$\hat{G}(p) = \frac{\hat{b}_m p^m + \hat{b}_{m-1}p^{m-1} + \dots \hat{b}_0}{p^n + \hat{a}_{n-1}p^{n-1} + \dots \hat{a}_0}, \quad (30)$$

$$\hat{u}(t) = \sum_{i=1}^M \hat{\gamma}_i h(t - \tau_i). \quad (31)$$

A. The BLSSVF Algorithm

To estimate the model parameters and the input signal, we propose Algorithm 1 which obtains an extended parameter vector (20) and then uses a rank-1 approximation (25) to separate the coupled parameters.

Algorithm 1 BLSSVF approach

1: Input: data $\{y(t_k)\}_{k=1}^N$, model $\{n, m\}$, SVF cutoff λ_{SVF}, CT function $h(t)$, translations $\{\tau_i\}_{i \geq 1}$.
2: Construct $y_f^{(i)}(t_k) \leftarrow \frac{p^{(i)}}{F(p)} y(t_k)$ ▷ Compute filtered time derivatives $\forall t_k \in \{t_1, \dots, t_N\}$
3: Compute $h_f^{(i)} \leftarrow \mathcal{L}^{-1}\left(\frac{p^{(i)}}{F(p)} \mathcal{L}(h) \right)$ ▷ $\mathcal{L}$ is the Laplace transform
4: Form regressor matrix structure from (17)
5: Compute (21) to obtain $\hat{\boldsymbol\theta}$
6: Construct $\hat{\mathbf{a}} \leftarrow \hat{\boldsymbol\theta}_{1:n}$
7: Form $\mathbf{Z}$ from using (24)
8: Obtain $[\hat{\mathbf{b}}, \hat{\mathbf{c}}]$ using (28)
9: Output: Model $\hat{G}(p)$ and input $\hat{u}(t)$ estimates using (30) and (31)

To provide theoretical support for Algorithm 1 we show that it satisfies the property of correctness [15]. We define correctness for a BSI algorithm (to take into account an estimate of the system up to a constant gain) as follows:

Definition 3.1: In BSI, an algorithm satisfies the property of correctness if the true model is estimated for $v(t) = 0$, given a finite amount of data N, that is, there exists some $N_0 < \infty$ such that

$$\alpha\hat{G}^N(p) = G^*(p) \quad \forall N \geq N_0, \quad (32)$$

where $\alpha \neq 0$ is a constant gain. Additionally, the input estimate $\hat{u}(t)$ must satisfy

$$\frac{1}{\alpha}\hat{u}(t) = u^*(t). \quad (33)$$

The following theorem provides proof that the proposed BLSSVF approach satisfies Definition 3.1. This relates to contribution (C2.a).

Theorem 3.1: Consider the continuous-time system (5). Let $\hat{G}^N(p)$ denote the estimate of the true system $G^*(p)$ for known numerator and denominator polynomials of orders n and m, respectively. Provided that the input is a linear combination of known functions $h(t)$, $F(p) = A^*(p)$, the normal matrix $(\varphi^\top\varphi)$ is nonsingular and $N_0 > n + (m + 1)M$, for a constant gain α then for all $N > N_0$,

$$\alpha\hat{G}^N(p) = G^*(p). \tag{34}$$

Consequently, the input estimate $\hat{u}(t)$ satisfies

$$\frac{1}{\alpha}\hat{u}(t) = u^*(t). \tag{35}$$

Proof: See Appendix VI-A. ∎

Remark 3.1: The nonsingularity of $(\varphi^\top\varphi)$ depends on the persistence of excitation of the input, as well as the sampling period of the output. A formal treatment of these conditions will be investigated in future work.

IV. SIMULATIONS

In this section the performance of the proposed estimator using Algorithm 1 is demonstrated via Monte Carlo simulations for contribution (C2.b). The system under study has the CT transfer function

$$G(p, \boldsymbol{\theta}^*) = \frac{b_1 p + b_0}{p^2 + a_1 p + a_0}, \tag{36}$$

where the true coefficients of the system are $\mathbf{b}^* = [1, 14]^\top$ and $\mathbf{a}^* = [8, 15]^\top$. The true input parameters, $\mathbf{c}^*$, are generated randomly from a normal distribution to persistently excite the system, and remain the same in all simulations. The simulation time was set to 24.6 seconds, where two data sets of $N = 1000$ and $N = 10000$ output samples were taken to identify the system, shown in Fig. 2 for one of the simulations.
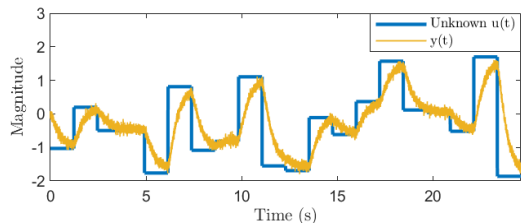

Fig. 2. Input-output data with u and y being the unknown input and measured output with a SNR of 20dB, from the system in (36).

The period T_u was set to 1.23 seconds which creates twenty equally spaced changes in the input signal, shown in Fig. 2. The simulation was repeated for output signal to noise ratios (SNRs) of 10, 20 and 40 dB, where different realisations of measurement noise were used for each simulation. Note that the input is shown here but it is not used in the estimation. As the input is assumed to be generated from a ZOH, $h(t)$ in Algorithm 1 is set to be a step function. Violin plots were utilised to display the results, as they convey the probability density of the data as well as standard statistical measures such as the mean, median, and outliers. As a result of Theorem 3.1, the estimates of $\mathbf{b}$ and $\mathbf{c}$ are scaled by a constant α and $1/\alpha$, respectively, so that the algorithm's performance could be assessed using violin plots. In the following experiments the effect of decreasing the number of

samples N whilst keeping the number of parameters constant is investigated. An output fit score [11], defined as

$$\text{Output Fit Score} = 1 - \frac{\|\hat{\mathbf{y}} - \mathbf{x}\|_2}{\|\mathbf{x} - \bar{\mathbf{x}}\|_2},$$

where $\hat{\mathbf{y}}$ and $\mathbf{x}$ are the predicted and noise-free outputs, and $\bar{\mathbf{x}}$ is the mean of $\mathbf{x}$, is used with the R-1 Fit (29) to demonstrate the performance of the algorithm.

A. Experiment 1: $N = 10000$

This experiment shows the performance of BLSSVF when $N = 10000$. At each SNR 100 Monte Carlo runs are conducted. The violin plots in Fig. 3 reveal that the blind approach performs well with the limited number of samples when the output SNR level is 40 dB, and performance decreases with lower SNRs. The R-1 Fit of $\mathbf{Z}$ improves as the output SNR increases as shown in Fig. 4.
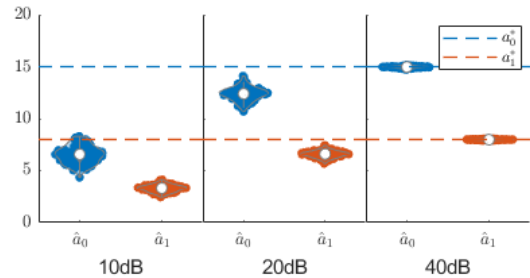

Fig. 3. Violin plot containing the estimation of $\hat{\mathbf{a}}$ for the Monte Carlo simulations where the output SNR is 10, 20, and 40 dB. N=10000
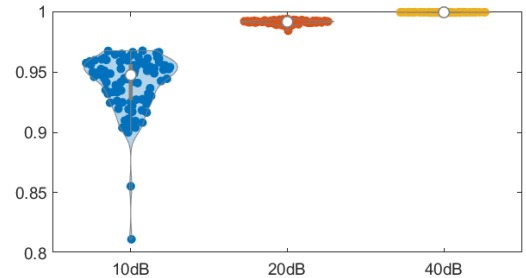

Fig. 4. Violin plot of the R-1 Fit computed in (29). The averages are 94.02%, 99.11% and 99.93% for output SNR's of 10, 20 and 40 dB. N=10000

Inevitably, as the rank-1 approximation improves so does the estimation of $\mathbf{b}$ and $\mathbf{c}$, shown in Figs. 5 and 6. Note that Fig. 6 shows the estimation error in $\mathbf{c}$. It is worth noting that forty-two parameters are estimated in step (5) of Algorithm 1 for this experiment with ten-thousand output data samples, which may not be enough to obtain a good model especially in the case of low output SNR's.
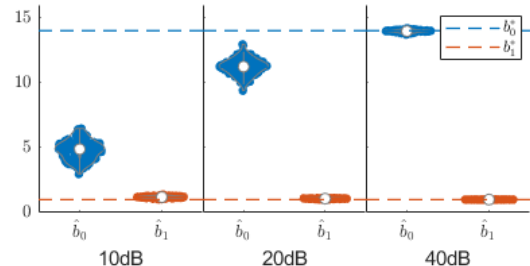

Fig. 5. Violin plot containing the estimation of $\hat{\mathbf{b}}$ for the Monte Carlo simulations for output SNR's of 10, 20 and 40 dB. N=10000.

The effects of applying the normalisation are shown in Fig. 6, where the first input parameter γ_1 has zero error as the estimates of **b** and **c** have been adjusted accordingly. These results show that an accurate system estimates can be obtained up to a scalar gain for high output SNR's.
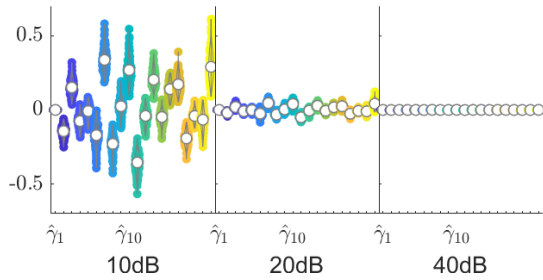

Fig. 6. Violin plot containing the estimation error of $\hat{\mathbf{c}}$ for the Monte Carlo simulations for output SNR's of 10, 20 and 40dB. Each ith x-axis tick indicates the estimation error for $\hat{\gamma}_i$. N=10000.

It is important to analyse the parameter estimates and not just the output fit scores. It is shown in Fig. 7 that even though the BLSSVF estimates are poor at 10 dB, the output fit score indicates a good fit.
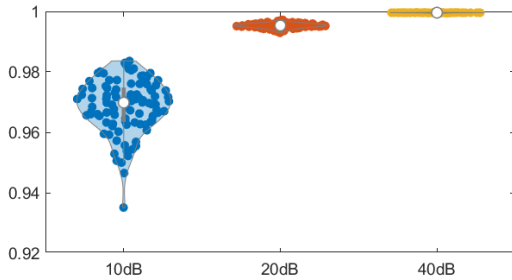

Fig. 7. Violin plot of output fit scores for output SNR's of 10, 20 and 40dB. The averages are 96.86%, 99.53% and 99.96% for output SNR's of 10, 20 and 40 dB. N=10000.

B. Experiment 2: $N = 1000$

This experiment is similar to that in Section IV-A, however, only one-thousand output data samples are now collected due to increasing the sampling period by a factor of ten whilst keeping the same duration of the experiment. In comparison to Figs. 3 and 5, Figs. 8 and 9 show that the parameter estimates of the model deteriorate with the decrease of samples, as would be expected. A similar observation can be made regarding Figs. 6 and 10, where the residual error between the true input parameters and $\hat{\mathbf{c}}$ from the output of Algorithm 1 are shown.
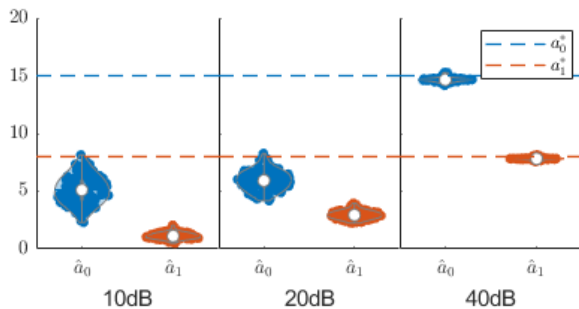

Fig. 8. Violin plot containing the estimation of $\hat{\mathbf{a}}$ for the Monte Carlo simulations where the output SNR is 10, 20, and 40 dB. N=1000.

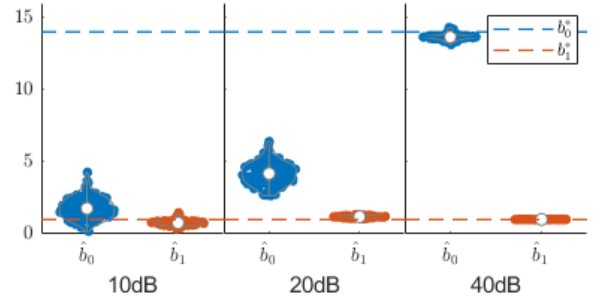Fig. 9. Violin plot containing the estimation of $\hat{\mathbf{b}}$ for the Monte Carlo simulations for output SNR's of 10, 20 and 40 dB. N=1000.

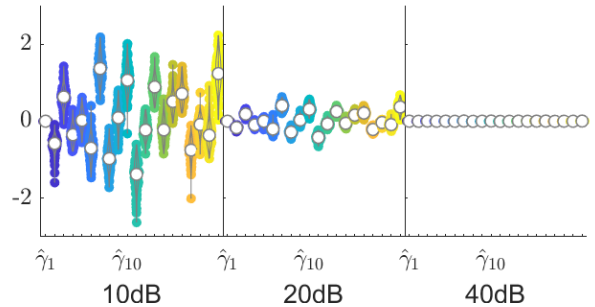Fig. 10. Violin plot containing the estimation error of $\hat{\mathbf{c}}$ for the Monte Carlo simulations for output SNR's of 10, 20 and 40 dB. N=1000. Notice the change of scale compared to Fig. 6

V. CONCLUSION

This paper presented a novel approach to blindly identify a LTI SISO system in a direct continuous-time form. Due to identifiability issues concerning blind identification problems, assumptions on the input were made where it is modelled by a linear combination of continuous-time functions. The proposed algorithm was proven to satisfy the correctness property given a sufficient number of data output samples under some mild conditions. The performance of the estimation improved as the output SNR increased as expected. Increasing the number of samples also reduced the error and the variation of the estimates.

VI. APPENDIX

A. Proof of Theorem 3.1

Proof: To prove that an algorithm blind to the input satisfies the correctness property, we must show that

$$\alpha \hat{G}(p) = G^*(p), \text{ and } \frac{1}{\alpha}\hat{u}(t) = u^*(t). \quad (37)$$

As the system and input are described by a parameter vector it is sufficient to show that

$$\hat{\boldsymbol{\theta}} - \boldsymbol{\theta}^* = \mathbf{0}. \quad (38)$$

Let us consider the matrix form of (16) for when $v(t) = 0$, i.e. $\mathbf{y}_f = \boldsymbol{\varphi}^*\boldsymbol{\theta}^*$, then the noiseless estimate of parameter vector in (15) is

$$\hat{\boldsymbol{\theta}} = (\boldsymbol{\varphi}^\top\boldsymbol{\varphi})^{-1}(\boldsymbol{\varphi}^\top\boldsymbol{\varphi}^*)\boldsymbol{\theta}^*. \quad (39)$$

To satisfy (38) we must show that $\boldsymbol{\varphi} = \boldsymbol{\varphi}^*$. Firstly, consider the true continuous-time model (8)

$$y(t) = \frac{B^*(p)}{A^*(p)} \sum_{i=1}^{M} \gamma_i^* h(t - \tau_i), \qquad (40)$$

where the noise $v(t) = 0$ and γ_i^* is the ith true input parameter. To find the true regressor we form $\boldsymbol{\theta}^*$ by multiplying (40) by $A^*(p)/F(p)$ and then expanding

$$y_f^{(n)}(t) + \sum_{i=0}^{n-1} a_i^* y_f^{(i)}(t) = \sum_{i=0}^{m} b_i^* u_f^{(i)}(t). \qquad (41)$$

We rearrange (41) into matrix form

$$y_f^{(n)}(t) = \varphi_f^\top(t)\boldsymbol{\theta}^*, \qquad (42)$$

where

$$\varphi_f(t) = \Big[-y_f^{(n-1)}(t), -y_f^{(n-2)}(t), \ldots, -y_f^{(0)}(t),$$
$$\mathbf{h}_f^{(m)}(t), \mathbf{h}_f^{(m-1)}(t), \ldots, \mathbf{h}_f^{(0)}(t)\Big]^\top,$$
$$\boldsymbol{\theta}^* = [\mathbf{a}^{*\top}, \mathbf{z}_m^{*\top}, \mathbf{z}_{m-1}^{*\top}, \ldots, \mathbf{z}_0^{*\top}]^\top. \qquad (43)$$

In relation to (22) and (23) we see in order to achieve $\boldsymbol{\theta}^*$ in (39) we must satisfy

$$\left\{y_f^{(l)}(t)\right\}_{t=t_k} = y_f^{(l)}(t_k), \qquad (44)$$

$$\left\{\frac{p^{(l)} A^*(p)}{F(p)} y(t)\right\}_{t=t_k} = \frac{p^{(l)} A^*(p)}{F(p)} y(t_k), \qquad (45)$$

which depends on the interpolation of the input and output. Given that $F(p) = A^*(p)$ and Assumption 3.2; then, (45) holds true when $l = 0$. For $l \geq 0$, $y_f^{(l)}(t_k)$ becomes an approximate of the true sampled filtered output derivative. However if we rearrange (16) in terms of $\epsilon(t_k)$ to yield the equivalent expressions

$$y_f^{(n)}(t_k) - \varphi_f^\top(t_k)\boldsymbol{\theta} = y(t_k) - \frac{B(p)}{A(p)} \sum_{i=1}^{M} \gamma_i h(t_k - \tau_i), \quad (46)$$

we see that the output intersample behaviour will not affect the overall estimation of $\hat{\boldsymbol{\theta}}$. Hence we have obtained

$$\hat{\boldsymbol{\theta}} = (\boldsymbol{\varphi}^{*\top} \boldsymbol{\varphi}^*)^{-1}(\boldsymbol{\varphi}^{*\top} \boldsymbol{\varphi}^*)\boldsymbol{\theta}^*. \qquad (47)$$

If we assume that the normal matrix $(\boldsymbol{\varphi}^{*\top} \boldsymbol{\varphi}^*)^{-1}$ is nonsingular, i.e. $N > n + (m + 1)M$, then (47) yields the true parameter under no noise. From (47) we thus obtain

$$\hat{\mathbf{a}} = \mathbf{a}^* \qquad (48)$$
$$\hat{\mathbf{z}}_i = \mathbf{z}_i^*, \qquad \text{for } i = 0, 1, \ldots m. \qquad (49)$$

Now, we must also show that the numerator coefficients $\hat{\mathbf{b}}$ can be extracted from the components of $\mathbf{z}$ up to a scalar gain $\alpha \in \mathbb{R}$. From (24) we have the relationship $\hat{\mathbf{Z}} = \mathbf{Z}^*$. The estimated parameter vectors $\hat{\mathbf{b}}$ and $\hat{\mathbf{c}}$ can be obtained from $\mathbf{Z}^*$. As $\mathbf{Z}^*$ is constructed from a row and column vector from the true parameters vector $\mathbf{b}^*$ and $\mathbf{c}^*$ then it has a rank of 1. Thus $\mathbf{Z}^*$ can be factorised up to a proportionality constant of the true parameter vectors. We can show this using a SVD, as the singular value matrix of rank-1 will have the form

$$\boldsymbol{\Sigma} = \begin{bmatrix} \sigma_1 & 0 & \ldots & 0 \\ 0 & 0 & \ldots & 0 \\ \vdots & \vdots & \ddots & \vdots \end{bmatrix} \in \mathbb{R}^{(m+1) \times M}. \qquad (50)$$

Then $\mathbf{U}_{(:,1)}$, $\mathbf{V}_{(:,1)}$ and σ_1 only need to be used to describe $\mathbf{Z}^*$, which are proportional to $\mathbf{b}^*$ and $\mathbf{c}^*$, respectively. Then

$$\hat{\mathbf{b}} = \mathbf{U}_{(:,1)} \sigma_1 \mathbf{V}_{(1,1)}, \text{ and } \hat{\boldsymbol{\gamma}} = \frac{\mathbf{V}_{(:,1)}}{\mathbf{V}_{(1,1)}}. \qquad (51)$$

If we consider that the proportional constant between the estimated and true vector is $\alpha = \hat{\gamma}_1$ (which is non-zero) we obtain

$$\hat{b}_i = b_i^* \hat{\gamma}_1, \text{ and } \hat{\gamma}_j = \gamma_j^* \frac{1}{\hat{\gamma}_1}, \qquad (52)$$

where $i = 1, 2, \ldots, m$ and $j = 1, 2, \ldots, M$. Thus $\hat{b}_i$ and $\hat{\boldsymbol{\gamma}}$ are proportionally equal to the true vectors up to a constant gain $\hat{\gamma}_1$. Substituting $\hat{\mathbf{a}}$ and $\hat{\mathbf{b}}$ into a transfer function form yields a scaled version of the true system

$$\hat{G}(p) = \hat{\gamma}_1 \frac{b_m^* p^m + b_{m-1}^* p^{m-1} + \ldots b_0^*}{p^n + a_{n-1}^* p^{n-1} + \ldots a_0^*}. \qquad (53)$$

The estimate of the input is then

$$\hat{u}(t) = \frac{1}{\hat{\gamma}_1} \sum_{i=1}^{M} \hat{\gamma}_i^* h(t - \tau_i). \qquad (54)$$

∎

REFERENCES

[1] L. Ljung, *System Identification: Theory for the User,* 2nd ed *Prentice-Hall*, 1998.

[2] G. Xu, H. Liu, L. Tong and T. Kailath, "A Least-Squares approach to Blind Channel Identification" *IEEE Transactions on Signal Processing*, vol. 43, no. 12, p 2982-2993, 1995.

[3] E. Bai, M. Fu, "Blind system identification and channel equalization of IIR systems without statistical information" *IEEE Transactions on Signal Processing*, vol. 47, no. 7, pp. 1910-1921, 1999.

[4] T. F. Chan, C. Wong, "Total Variation Blind Deconvolution" *IEEE Transactions on Image Processing*, vol. 7, no. 3, pp. 370-375, 1998.

[5] W. Liu, Z. Li, Y. Wang, D. Song, N. Ji, L. Xu, T. Mei, Y. Sun and S. E. Greenwald, "Aortic pressure waveform reconstruction using a multichannel Newton blind system identification algorithm" *Computers in Biology and Medicine*, vol. 135, pp. 104545, 2021.

[6] K. Abed-Meraim, W. Qui and Y. Hua, "Blind system identification" *Proceedings of the IEEE*, vol. 85, no. 8, pp. 1310-1322, 1997.

[7] Y. Hua, "Blind methods of system identification" *Circuits Systems Signal Processing*, vol. 21, no. 1, pp. 91-108, 2022.

[8] H. Garnier and P. C. Young, "The advantages of directly identifying continuous-time transfer function models in practical applications" *International Journal of Control*, vol. 87, no. 7, p 1319-1338, 2013.

[9] B. Wahlberg, "The effects of rapid sampling in system identification" *Automatica*, vol. 26, no. 1, pp. 167-170, 1990.

[10] H. Garnier, L. Wang and P. C. Young, "Direct identification of continuous-time Models from Sampled Data: issues, basic solutions and relevance" *Springer*, vol. 21, no. 1, p 1-29, 2008.

[11] G. Bottegal, R. S. Risuleo and H. Hjalmarsson, "Blind system identification using kernel-based methods" *IFAC-PapersOnLine*, vol. 48, no. 12, pp. 446-471, 2015.

[12] P. C. Young, "Process parameter estimation and self adaptive control" *IFAC Proceedings Volumes*, vol. 2, no. 2, pp. 118-140, 1965.

[13] E. Bai, "An optimal two-stage identification algorithm for Hammerstein–Wiener nonlinear systems" *Automatica*, vol. 34, no. 3, pp. 333-338, 1998.

[14] S. Pan, J. S. Welsh, R. A. Gonzalez and C. R. Rojas, "Consistency analysis and bias elimination of the Instrumental-Variable-based State Variable Filter method" *Automatica*, vol. 144: 110511, 2022.

[15] T. McKelvey, H. Akçay and L. Ljung, "Subspace-based multivariable system identification from frequency response data" *IEEE Transactions on Automatic control*, vol. 41, no. 7, pp. 960-979, 1996.